HHS Public Access

Author manuscript

Nature. Author manuscript; available in PMC 2012 November 03.

Published in final edited form as:

Nature. 2012 May 3; 485(7396): 133–136. doi:10.1038/nature10994.

Stereospecific binding of a disordered peptide segment mediates BK channel inactivation

Vivian Gonzalez-Perez[1,*], **Xu-Hui Zeng**[1,*,$], **Katie Henzler-Wildman**[2], and **Christopher J. Lingle**[1,+]

[1]Department of Anesthesiology, Washington University School of Medicine, St. Louis MO, USA

[2]Department of Biochemistry, Washington University School of Medicine, St. Louis, MO USA

Keywords

K^+ channels; inactivation mechanisms; N-terminal inactivation domains; BK channels; Ca^{2+}- and voltage-gated K^+ channels; *Slo* channels

Introduction

A number of functionally important actions of proteins are mediated by short intrinsically disordered peptide segments[1], but the molecular interactions that allow disordered domains to mediate their effects remain a topic of active investigation[2–5]. Many K^+ channel proteins, following initial channel opening, exhibit a time-dependent reduction in current flux, termed inactivation, that involves movement of mobile cytosolic peptide segments (~20–30 residues) into a position that physically occludes ion permeation[6–8]. Peptide segments that produce inactivation exhibit little amino acid identity[6,9–13] and tolerate appreciable mutational substitutions[13] without disrupting the inactivation process. Solution NMR of several isolated inactivation domains reveals substantial conformational heterogeneity with only minimal tendency to ordered structures[14–17]. Channel inactivation mechanisms may therefore be informative regarding how intrinsically disordered regions mediate functional effects. Whereas many aspects of inactivation of voltage-dependent K^+ channels (Kv) can be well-described by a simple one-step occlusion mechanism[6,7,18,19], inactivation of the Ca^{2+}- and voltage-dependent BK K^+ channel mediated by peptide segments of auxiliary β subunits involves two distinguishable kinetic steps[20,21]. Here, we show that two-step inactivation mediated by an intrinsically disordered BK β subunit peptide involves a stereospecific binding interaction that precedes blockade. In contrast, block mediated by a *Shaker* Kv inactivation peptide is consistent with direct, simple occlusion by a hydrophobic segment without substantial steric requirement. The results indicate that two distinct types of

[+]Correspondence to C.J Lingle. clingle@morpheus.wustl.edu.

[*]These authors contributed equally to this work.

[$]Present address: Institute of Life Science, Nanchang University, 999 Xuefu Road, Honggu District, Nanchang, China 33031

V.G.P. and X.Z. designed experiments, and collected and analyzed data. K.H.W. performed or supervised CD and NMR determinations; C.L. conceived the project, designed research, analyzed data, and prepared the manuscript.

molecular interactions between disordered peptide segments and their binding sites produce qualitatively similar functions.

For BK channels, inactivation is mediated by cytosolic N-terminal segments of auxiliary β subunits (Fig. S1a)[20–24]. In contrast to simple models proposed for Kv N-type inactivation ($C \leftrightharpoons O \leftrightharpoons I$), for BK β subunits the mechanism of inactivation involves two steps[20,21] ($C \leftrightharpoons O \leftrightharpoons O^* \leftrightharpoons I^*$), an initial transition to a preinactivated conducting state (O*) followed by transition to a non-conducting inactivated state (I*) (Fig. S2a). The properties of inactivation onset and recovery differ among subunits[20–24], presumably dependent on the interactions of each β subunit N-terminus and the BK α subunit. The site(s) and physical basis for this sequence of steps in BK inactivation are not understood. Here we exploit inactivation mediated by the BK β3a subunit to tease apart the molecular steps in two-step inactivation[21]. First, both the β3a subunit (Fig. 1a) and a β3a peptide (Fig. 1b) produce a slowing of BK tail currents which arises from buffering of channels between $O^* \leftrightharpoons I^*$[21]. Net current flux during the tail current greatly exceeds that expected for a population of open BK channels simply passing back to closed states[21] (Fig. 1a,b). Second, the unique properties of the $O^* \leftrightharpoons I^*$ equilibrium can be directly visualized in recordings of single BK channels during recovery from inactivation mediated either by β3a N-termini[21] or by β3a peptides (Fig. 1c). Following repolarization, inactivated single channels open to a current level of reduced amplitude, higher variance, and longer duration than a typical BK channel closing (Fig. 1c). The lower current level is a direct reflection of the rapid voltage-dependent equilibrium between states O* and I* (Fig. S2). Since the isolated β3a peptide mimics the effects of the tethered β3a N-terminus (Fig 1a–c), the peptide can be exploited for examination of the structural and functional basis of the two-step mechanism. CD spectra of both a β3a peptide composed of the naturally occurring L-amino-acids and an unnatural, mirror-image peptide composed of D-amino acid enantiomers (Fig. 1d) are typical of random coil and an absence of secondary structure. Solution NMR spectra of these two peptides are identical and exhibit minimal chemical shift dispersion (Fig. 1e, S3a). The peptides also exhibit very few inter-residue NOEs in 2D homonuclear NOESY spectra (Fig. S3b), consistent with intrinsic disorder.

We hypothesize that the two-step process involves a binding step that precedes rapid motions of a flexible part of the bound N-terminus in and out of a position of pore occlusion. If binding has a unique steric requirement (stereospecific binding), a β3a peptide composed entirely of D-amino acids should fail to interact with this site. Both 21-mer L- and D-amino acid β3a peptides produced block of BK current (Fig. 2a,d), with block by the D-peptide of lower affinity (Fig. S4). However, the D-peptide (Fig. 2e–f) failed to mimic the ability of the L-peptide (Fig. 2b–c) to slow the tail current decay and increase tail current flux.

Since the D-peptide acts with lower affinity, the differential effects of the two peptides might arise, not from a difference in underlying mechanism, but because the O* state lifetime involving the D-peptide may be too brief to resolve. We therefore compared the ability of L- and D-peptides to block single channel BK openings (Fig. 2g). With 10 μM D-peptide, frequent unblocking events are observed, consistent with its weaker affinity. Following repolarization, a channel blocked by the L-peptide exhibits rapid unblock to the reduced current level, before unblock to a full BK open level. In contrast, a channel blocked

by the D-peptide reopens to a full current level, with no hint of the reduced current level seen with the L-peptide. When examined at higher time resolution (Fig. 2h), repolarization following L-peptide block resulted in an essentially instantaneous step to the level of reduced current, consistent with the properties of the O*-I* equilibrium (Fig. S2d–f). Repolarization following D-peptide block revealed a finite delay prior to a full BK opening (Fig. 2h), similar to block of Kv channels[18]. The differential effects of the peptides show that stereospecific binding of L-peptide is required to produce the tail current prolongation. Although the steric binding occurs even in the absence of intrinsic structure in the free peptide, it would not be surprising that, once bound, the peptide adopts a specific structure. We also found that inactivation produced by a β3a N-terminus (β3a-R16Q/R17Q/R18Q) in which the first 20 residues are uncharged (Fig. S5) retains the slow tail currents and single channel openings indicative of two-step inactivation. We conclude that the binding event underlying the O* state depends on hydrophobic interactions with unique steric requirements without significant contribution from electrostatic effects.

If the D-peptide blocking events arise from relatively non-specific binding, not requiring a specific steric fit but dependent on bulk hydrophobicity, the L-peptide should occasionally act in a similar fashion, in accordance with relative occupancies of non-specific and stereospecific sites. For a set of single BK channel tail openings in the presence of 10 μM β3a L-peptide, ~3% of tail current reopenings occurred with a well-defined latency prior to opening to a full open channel level; openings to a reduced current level with no latency were ~30-fold more abundant (Fig. S6a,b). Thus, the BK channel can be blocked in two distinct ways by the β3a L-peptide. The more common reopening to the reduced current level (O*-I*) is only observed with the L-peptide. However, reopening to a fully open level is observed more rarely with L-peptide, and this behavior is similar to the one-step block (O-I) characteristic of the β3a D-peptide or block of the *Shaker* channel[18]. Since recovery from I* is much more rapid (Fig. S2) than for the rarer form of block (O-I), the peptide position within the channel must in each case differ markedly.

We next asked whether peptide blockade of *Shaker* Kv channels may exhibit a similar steric dependence. *Shaker* inactivation peptides, which also exhibit little defined structure[14], tolerate appreciable amino acid substitution without altering inactivation as long as bulk hydrophobicity is maintained[13]. If block largely reflects bulk hydrophobicity with no steric requirement, L- and D- *Shaker* peptides should show similar block affinities and kinetics. Tests of 20-mer L- and D- *Shaker* peptides on *Shaker*(Δ2-46) channels confirmed this expectation with little difference in blocking affinity (Fig. 3a–d; Fig. S7). Unblock from either peptide occurred in a fashion consistent with a single-step occlusion mechanism not dependent on stereochemistry (Fig. 3e,f). Thus, the key determinants that define block behavior of the *Shaker* ball peptide within the *Shaker* inner pore do not include a steric interaction. However, this does not exclude that a *Shaker* peptide might electrostatically interact with positions that may influence block affinity[13,25] or that a form of two-step inactivation also proposed in Kv channels[8,25] may occur (see Supplementary Text).

Our results do not identify the location of the β3a L-peptide binding site. For Shaker K^+ channels, the ability of TEA to slow inactivation onset argues that TEA and the *Shaker* N-terminus compete for a common position within the inner pore[26]. For BK inactivation, the

inability of pore blockers to interfere with inactivation onset is a natural consequence of the two-step inactivation mechanism[20]. If a fast blocker binds with similar affinity to both O and O* states and the rate-limiting inactivation step is the transition from O to O*, even if a blocker competitively inhibits movement of an inactivation domain into a position of inactivation, it will not slow the onset of inactivation (Fig. 4). However, the effects of blockers on slow tail current allow mechanistically informative tests regarding the interactions of pore blockers and the inactivation domain (Fig. S8). We considered three cases: one in which blocker competitively impedes formation of O* and subsequently I* (Fig. S8a, Model 1), one in which blocker does not impede any aspect of the inactivation process (Fig. S8a, Model 2), and two variants of a model (Fig. S8a, Models 3 and 3') in which block competitively inhibits inactivation. Each scheme results in distinct predictions regarding blocker effects on the time course of β3a-mediated currents, both for onset of inactivation (Fig. S8b,d) and for tail currents (Fig. S8c,d). Only the model (Model 3) in which a pore blocker competitively prevents the $O^* \rightarrow I^*$ transition predicts that blocker will reduce both tail current amplitude and duration (Fig. 4a,b).

We therefore tested the effects of the pore blocker, TBA[27], on β3a-mediated tail currents; both peak tail current and tail current time constant were reduced (Fig. 4c,d). These effects occur at concentrations in excess of the TBA blocking affinity for open BK channels (~0.9 mM[27]), but consistent with the competitive model (Fig. 4b). Similar results were obtained with the bulky blocker, bbTBA[28] (Fig. 4e,f). We conclude that β3a-mediated inactivation involves movement of part of the β3a N-terminus into a position that can also be occupied by BK pore blockers. Although it has been assumed that BK β subunit N-termini produce inactivation by occupying a site within the BK channel central cavity, this provides the first direct evidence of this assumption. Our results do not establish the position of the stereospecific interaction between β3a peptide and the α subunit, but we suggest that the binding site determinants are on the walls of the cavernous BK inner pore[29,30].

These results demonstrate at the single molecule level that an intrinsically disordered peptide domain can bind in a stereospecific fashion to a target protein, thereby mediating physiological effects. An important implication of the mechanism by which the β3a N-terminus prolongs tail current is that the O* state, although an open, ion-conducting conformation, is unable to close until the β3a peptide dissociates from the channel. We propose that not only does this intrinsically disordered peptide bind to a stereospecific site on or near the BK channel inner pore, but that binding allosterically stabilizes the BK channel in an open conformation. The requirement for stereospecific binding in BK inactivation contrasts with *Shaker* inactivation, which is mediated largely by hydrophobic interactions of its inactivation domain with the *Shaker* pore. In each case, inactivation domain disorder may be required to facilitate movement of the N-terminal inactivation segment through narrow pathways to reach blocking positions. The differences in stereochemical requirements may be required by structural differences in the ion channel pores: the *Shaker* domain may fit more snugly in the narrower open Kv channel[8], while in the larger BK channel inner pore[30] stereospecific binding may be required to achieve the affinity necessary for inhibition or to modulate channel gating.

Methods Summary

Recordings of channel activity utilized inside-out patches from *Xenopus* oocytes expressing either wt BK channels along with wt or mutant β3a subunits or *Shaker*-IR channels. All recordings were with symmetrical K^+ solutions, with solutions of calibrated Ca^{2+} applied to the cytosolic face of BK channels. Solution control and exchange at the cytosolic face of a patch were done with a multi-barrel pipette. Currents were typically acquired at 100 kHz sampling with filtering at 10 kHz. Single channel records utilized off-line subtraction based on null-sweeps. D- and L-peptides for β3a N-termini (MQPFSIPVQITLQGSRRRQGR-NH2) or Shaker N-termini MAAVAGLYGLGEDRQHRKKQ-NH2) were obtained commercially. Simulations of different models of inactivation utilized the IChSim program. 21-mer D- and L-β3a peptides were dissolved at a final peptide concentration of 2 mM for acquisition of 1D proton spectra and 2D homonuclear phase-sensitive TOCSY, NOESY, and ROESY spectra. CD spectra were generated with a Jasco J715 following dilution of the NRM samples in water.

Materials and Methods

Constructs

The mSlo1 construct (GenBank accession number NP_034740) was placed in the pXMX expression construct[31]. The mouse β3a construct (GenBank accession number NP_001182003.1) was described in previous work[32]. In some experiments, construct D20A, in which the human β3a N-terminus was attached to a human β2 construct (N-terminal removed), was used[21]. This construct avoids the outward rectification that arises from the extracellular loop of the β3 subunit[33]. The D20A N-terminus begins with 55 residues from human β3a that are then appended to human β2 beginning at the β2 first transmembrane segment (hβ3a:1-55);(hβ2:47-235). A *Shaker*-B construct was kindly provided by Dr. Lily Jan[34] and residues 2-46 of the N-terminus were deleted by Dr. Xiao-Ming Xia (Dept. Anesthesiology, Washington University-St. Louis) to generate the non-inactivating ShakerB(Δ2-46).

Heterologous expression in oocytes

Stage IV *Xenopus laevis* oocytes were used for expression of Slo1 and β3a constructs. Slo1 α and β3 cRNA, prepared at ~1 μg/μl, were first diluted to 1:20 and 1:10, respectively, and the diluted solutions mixed in equal amounts. Assuming that the initial β subunit RNA stock is ~3-4-fold higher molar amount than the Slo1 RNA stock, the final injection β3a:α molar injection ratio is ~6-8:1. For single channel patches, the amount of injected RNA was reduced about 10–100-fold.

Electrophysiology

Borosilicate capillary tubes (Drummond Microcaps, 100 μl) were pulled to diameters resulting in access resistance of 1–2 MΩ, coated with Sylgard (Sylgard 184, Dow Chemical Corp.) and fire-polished. Currents were recorded in the inside-out configuration[35] using an Axopatch 200 amplifier (Molecular Devices, Sunnyvale, CA) and the Clampex program from the pClamp software package (Molecular Devices).

Patches with gigaohm seals were formed in normal frog Ringer (in mM, 115 NaCl, 2.5 KCl, 1.8 CaCl2, 10 HEPES, pH 7.4) and then, after excision, moved into flowing test solutions to control the solution bathing the membrane face. The pipette/extracellular solution was (in mM): 140 K-methanesulfonate, 20 KOH, 10 HEPES, 2 MgCl2, pH 7.0. Test solutions bathing the cytoplasmic face of the patch membrane contained (in mM) 140 K-methanesulfonate, 20 KOH, 10 HEPES, with pH adjusted to 7.0 KOH. 5 mM HEDTA was used for 10 μM Ca^{2+} solutions and 5 mM EGTA for 0 μM Ca^{2+}. The 10 μM Ca^{2+} solution was titrated to appropriate pCa with Ca-MES and calibrated against solutions of defined Ca^{2+} concentrations (World Precision Instruments) using a Ca^{2+}-sensitive electrode. Solutions bathing the cytosolic face of the membrane were controlled by a local application system containing up to six independent lines. Experiments were at room temperature (22–24°C) and chemicals for solution preparation were from Sigma.

Data Analysis

Analysis of current recordings and simulated currents were accomplished either with Clampfit (Molecular Devices) or with programs written in this laboratory. Single channel traces were first processed utilizing digital subtraction of leak and capacity currents defined from traces lacking any channel openings. For ensemble averaging of *Shaker* single channel openings, each sweep was first filtered at 1 kHz (acquisition at 50 kHz with filtering at 5 kHz).

Simulation of currents

Current simulations were accomplished with the IChSim program (http://www.ifisica.uaslp.mx/~jadsc/ichsim.htm) developed at the Physics Institute of the University of San Luis Potosi, Mexico by Dr. Jose Antonio De Santiago Castillo.

Solution NMR

21-mer D- and L- β3a peptides were dissolved in 20 mM potassium phosphate, 20 mM sodium chloride, pH 7.0, 10% D2O with a final peptide concentration of 2 mM. 1D proton spectra and 2D homonuclear phase-sensitive TOCSY, NOESY, and ROESY spectra were recorded on a 600 MHz Bruker Avance III spectrometer equipped with QCI cryoprobe. NOESY and ROESY spectra were acquired with a mixing time of 300 ms, TOCSY with an 80 ms mixing time. All 2D homonuclear experiments were acquired with 512 points in the indirect dimension, and 16 scans per increment. Spectra were processed with NMRpipe and displayed using NMRViewJ (2D spectra) or IgorPro (1D spectra).

Circular Dichroism Spectra

The NMR samples were diluted 40-fold in water for measurement of CD spectra using a Jasco J715.

Peptides

L- and D-amino acid β3a peptides and L- and D-20-mer *Shaker*B ball peptides were custom synthesized by Biomolecules Midwest Inc. (Waterloo, IL) with an amidated C-terminus and NH2- N-terminus, and purified by HPLC to over 95% purity. Both 20 and 21 L-amino acid

versions of the β3a peptides were used in separate experiments. The 21-mer β3a peptide contains an additional R in position 21 and exhibits a faster forward rate of block than the 20-mer. The sequence of the 20-mer *Shaker*B ball peptides was MAAVAGLYGLGEDRQHRKKQ-NH2, identical to +2 *Shaker*B peptides utilized in previous work[6,13].

Supplementary Material

Refer to Web version on PubMed Central for supplementary material.

Acknowledgments

This work was supported by GM-081748 to CJL and the Searle Scholars Program to KHW. We thank Emma Morrison and Dr. Paul Schlesinger for assistance with dynamic light scattering measurements and Drs. Carl Frieden and Kanchan Garai for assistance with CD spectroscopy. We thank Hai Jiang, Alex Scott, and Jenny Jones for care of oocytes, and Drs. Joe Henry Steinbach and Rohit Pappu for comments on the manuscript.

Abbreviations used in this paper

BK	large conductance Ca^{2+}-activated K^+ channel
TEA	tetraethylammonium
TBA	tetrabutylammonium

References

1. Dyson HJ. Expanding the proteome: disordered and alternatively folded proteins. Q Rev Biophys. 2011:1–52.
2. Sugase K, Dyson HJ, Wright PE. Mechanism of coupled folding and binding of an intrinsically disordered protein. Nature. 2007; 447:1021–1025. [PubMed: 17522630]
3. Galea CA, et al. Role of intrinsic flexibility in signal transduction mediated by the cell cycle regulator, p27 Kip1. J Mol Biol. 2008; 376:827–838. [PubMed: 18177895]
4. Tompa P, Fuxreiter M. Fuzzy complexes: polymorphism and structural disorder in protein-protein interactions. Trends Biochem Sci. 2008; 33:2–8. [PubMed: 18054235]
5. De Sancho D, Best RB. Modulation of an IDP binding mechanism and rates by helix propensity and non-native interactions: association of HIF1alpha with CBP. Mol Biosyst. 2012; 8:256–267. [PubMed: 21892446]
6. Hoshi T, Zagotta WN, Aldrich RW. Biophysical and molecular mechanisms of Shaker potassium channel inactivation. Science. 1990; 250:533–538. [PubMed: 2122519]
7. Zagotta WN, Hoshi T, Aldrich RW. Restoration of inactivation in mutants of Shaker potassium channels by a peptide derived from ShB. Science. 1990; 250:568–571. [PubMed: 2122520]
8. Zhou M, Morais-Cabral JH, Mann S, MacKinnon R. Potassium channel receptor site for the inactivation gate and quaternary amine inhibitors. Nature. 2001; 411:657–661. [PubMed: 11395760]
9. Ruppersberg JP, Frank R, Pongs O, Stocker M. Cloned neuronal IK(A) channels reopen during recovery from inactivation [see comments]. Nature. 1991; 353:657–660. [PubMed: 1922383]
10. Tseng-Crank J, Yao JA, Berman MF, Tseng GN. Functional role of the NH2-terminal cytoplasmic domain of a mammalian A- type K channel. J Gen Physiol. 1993; 102:1057–1083. [PubMed: 7907648]
11. Rasmusson RL, Wang S, Castellino RC, Morales MJ, Strauss HC. The beta subunit, Kv beta 1.2, acts as a rapid open channel blocker of NH2-terminal deleted Kv1.4 alpha-subunits. Adv Exp Med Biol. 1997; 430:29–37. [PubMed: 9330716]

12. Kondoh S, Ishii K, Nakamura Y, Taira N. A mammalian transient type K^+ channel, rat Kv1.4, has two potential domains that could produce rapid inactivation. J Biol Chem. 1997; 272:19333–19338. [PubMed: 9235930]
13. Murrell-Lagnado RD, Aldrich RW. Interactions of amino terminal domains of Shaker K channels with a pore blocking site studied with synthetic peptides. J Gen Physiol. 1993; 102:949–975. [PubMed: 8133245]
14. Schott MK, Antz C, Frank R, Ruppersberg JP, Kalbitzer HR. Structure of the inactivating gate from the Shaker voltage gated K^+ channel analyzed by NMR spectroscopy. Eur Biophys J. 1998; 27:99–104. [PubMed: 9530825]
15. Wissmann R, et al. NMR structure and functional characteristics of the hydrophilic N terminus of the potassium channel beta-subunit Kvbeta1.1. J Biol Chem. 1999; 274:35521–35525. [PubMed: 10585425]
16. Wissmann R, et al. Solution structure and function of the "tandem inactivation domain" of the neuronal A-type potassium channel Kv1.4. J Biol Chem. 2003; 278:16142–16150. [PubMed: 12590144]
17. Bentrop D, Beyermann M, Wissmann R, Fakler B. NMR structure of the "ball-and-chain" domain of KCNMB2, the beta 2-subunit of large conductance Ca^{2+}- and voltage-activated potassium channels. J Biol Chem. 2001; 276:42116–42121. [PubMed: 11517232]
18. Demo SD, Yellen G. The inactivation gate of the Shaker K^+ channel behaves like an open- channel blocker. Neuron. 1991; 7:743–753. [PubMed: 1742023]
19. Gonzalez C, Lopez-Rodriguez A, Srikumar D, Rosenthal JJ, Holmgren M. Editing of human K(V)1.1 channel mRNAs disrupts binding of the N-terminus tip at the intracellular cavity. Nat Commun. 2011; 2:436. ncomms1446 [pii]. 10.1038/ncomms1446 [PubMed: 21847110]
20. Lingle CJ, Zeng XH, Ding JP, Xia XM. Inactivation of BK channels mediated by the N-terminus of the β3b auxiliary subunit involves a two-step mechanism: possible separation of binding and blockade. J Gen Physiol. 2001; 117:583–605. [PubMed: 11382808]
21. Zeng X-H, Xia XM, Lingle CJ. BK Channels with β3a subunits generate use-dependent slow afterhyperpolarizing currents by an inactivation-coupled mechanism. J Neurosci. 2007; 27
22. Xia XM, Ding JP, Lingle CJ. Molecular basis for the inactivation of Ca^{2+}- and voltage-dependent BK channels in adrenal chromaffin cells and rat insulinoma tumor cells. J Neurosci. 1999; 19:5255–5264. [PubMed: 10377337]
23. Wallner M, Meera P, Toro L. Molecular basis of fast inactivation in voltage and Ca^{2+}-activated K^+ channels: a transmembrane beta-subunit homolog. Proc Natl Acad Sci U S A. 1999; 96:4137–4142. [PubMed: 10097176]
24. Xia XM, Ding JP, Zeng XH, Duan KL, Lingle CJ. Rectification and rapid activation at low Ca^{2+} of Ca^{2+}-activated, voltage-dependent BK currents: consequences of rapid inactivation by a novel β subunit. J Neurosci. 2000; 20:4890–4903. [PubMed: 10864947]
25. Prince-Carter A, Pfaffinger PJ. Multiple intermediate states precede pore block during N-type inactivation of a voltage-gated potassium channel. J Gen Physiol. 2009; 134:15–34. [PubMed: 19528261]
26. Choi KL, Aldrich RW, Yellen G. Tetraethylammonium blockade distinguishes two inactivation mechanisms in voltage-activated K^+ channels. Proc Natl Acad Sci U S A. 1991; 88:5092–5095. [PubMed: 2052588]
27. Li W, Aldrich RW. Unique inner pore properties of BK channels revealed by quaternary ammonium block. J Gen Physiol. 2004; 124:43–57. [PubMed: 15197222]
28. Wilkens CM, Aldrich RW. State-independent Block of BK Channels by an Intracellular Quaternary Ammonium. J Gen Physiol. 2006; 128:347–364. [PubMed: 16940557]
29. Brelidze TI, Magleby KL. Probing the geometry of the inner vestibule of BK channels with sugars. J Gen Physiol. 2005; 126:105–121. [PubMed: 16043773]
30. Zhou Y, Xia XM, Lingle CJ. Cysteine scanning and modification reveal major differences between BK channels and Kv channels in the inner pore region. Proc Natl Acad Sci U S A. 2011; 108:12161–12166. [PubMed: 21730134]
31. Tang Q, Zeng XH, Lingle CJ. Closed channel block of BK potassium channels by bbTBA requires partial activation. J Gen Physiol. 2009; 134:409–436. [PubMed: 19858359]

32. Zeng X, Xia XM, Lingle CJ. Species-specific differences among KCNMB3 BK ß3 auxiliary subunits: some ß3 variants may be primate-specific subunits. J Gen Physiol. 2008; 132:115–129. [PubMed: 18591419]

33. Zeng XH, Xia XM, Lingle CJ. Redox-sensitive extracellular gates formed by auxiliary beta subunits of calcium-activated potassium channels. Nat Struct Biol. 2003; 10:448–454. [PubMed: 12740608]

34. Timpe LC, et al. Expression of functional potassium channels from Shaker cDNA in Xenopus oocytes. Nature. 1988; 331:143–145. [PubMed: 2448636]

35. Hamill OP, Marty A, Neher E, Sakmann B, Sigworth FJ. Improved patch-clamp techniques for high-resolution current recording from cells and cell-free membrane patches. Pflugers Archiv. 1981; 391:85–100. [PubMed: 6270629]

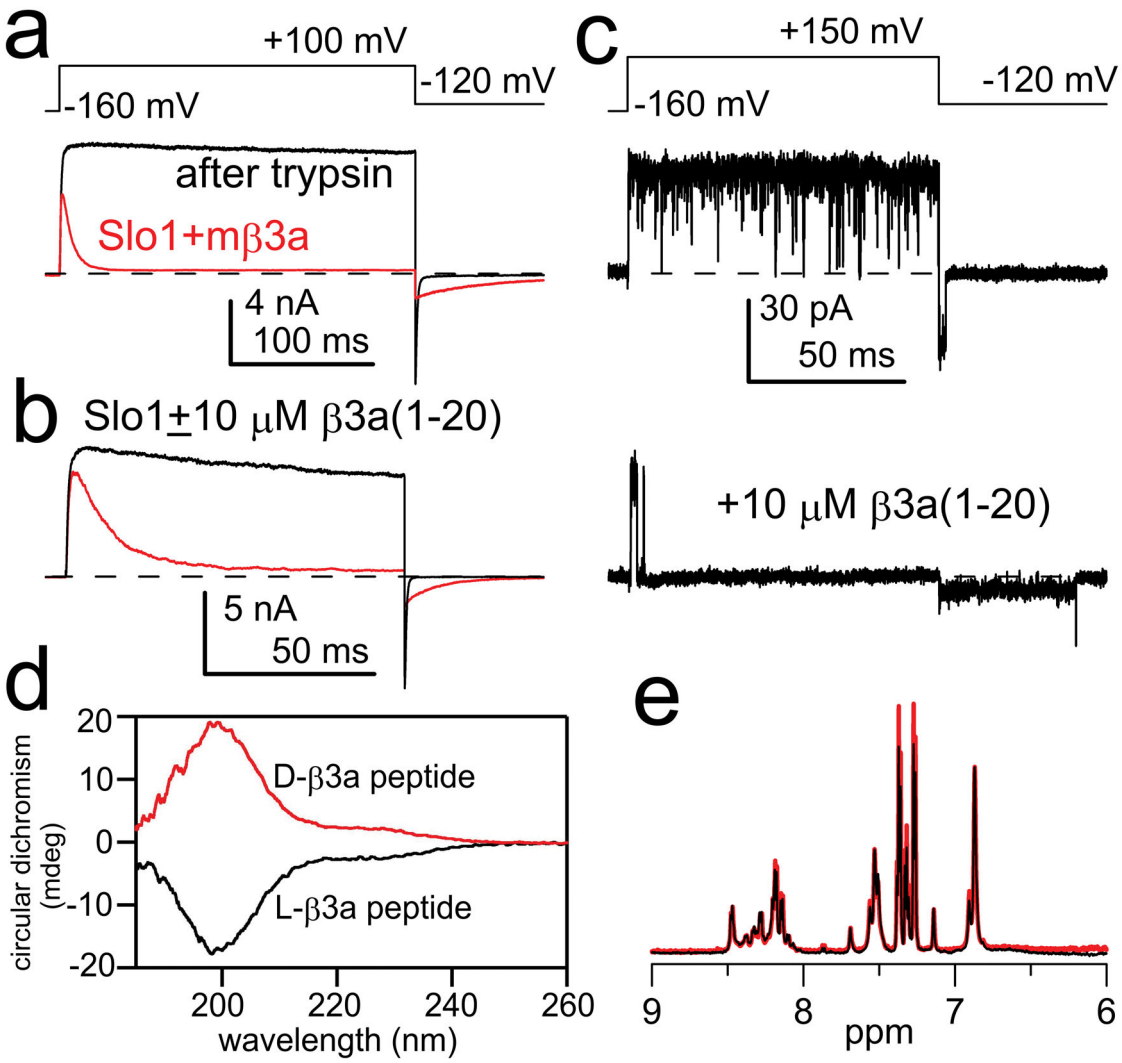

Figure 1. Intrinsically disordered β3a-N-terminal peptide mimics the two-step inactivation produced by the tethered β3a N-terminus

(a) Intact β3a subunits mediate trypsin-sensitive inactivation and tail current prolongation of BK channels. Red trace: BK α+β3a currents with the indicated protocol and 10 μM Ca^{2+}; black trace: after trypsin. **(b)** β3a(1-20) peptide (red) produces inactivation and slows BK tail currents. **(c)** Single BK channel in the absence (upper) and presence (lower) of β3a(1-20) peptide. Peptide produces block and a noisy long duration low amplitude openings prior to unblock. **(d)** Circular dichroism spectra of L- (black) and D- β3a-peptides (red) are identical except for expected opposite sign. Minimum below 200 nm is characteristic of random coil conformation. **(e)** Solution NMR of β3a 21-mer peptides (black: L-peptide; red: D-peptide) shows minimal chemical shift dispersion in the amide region.

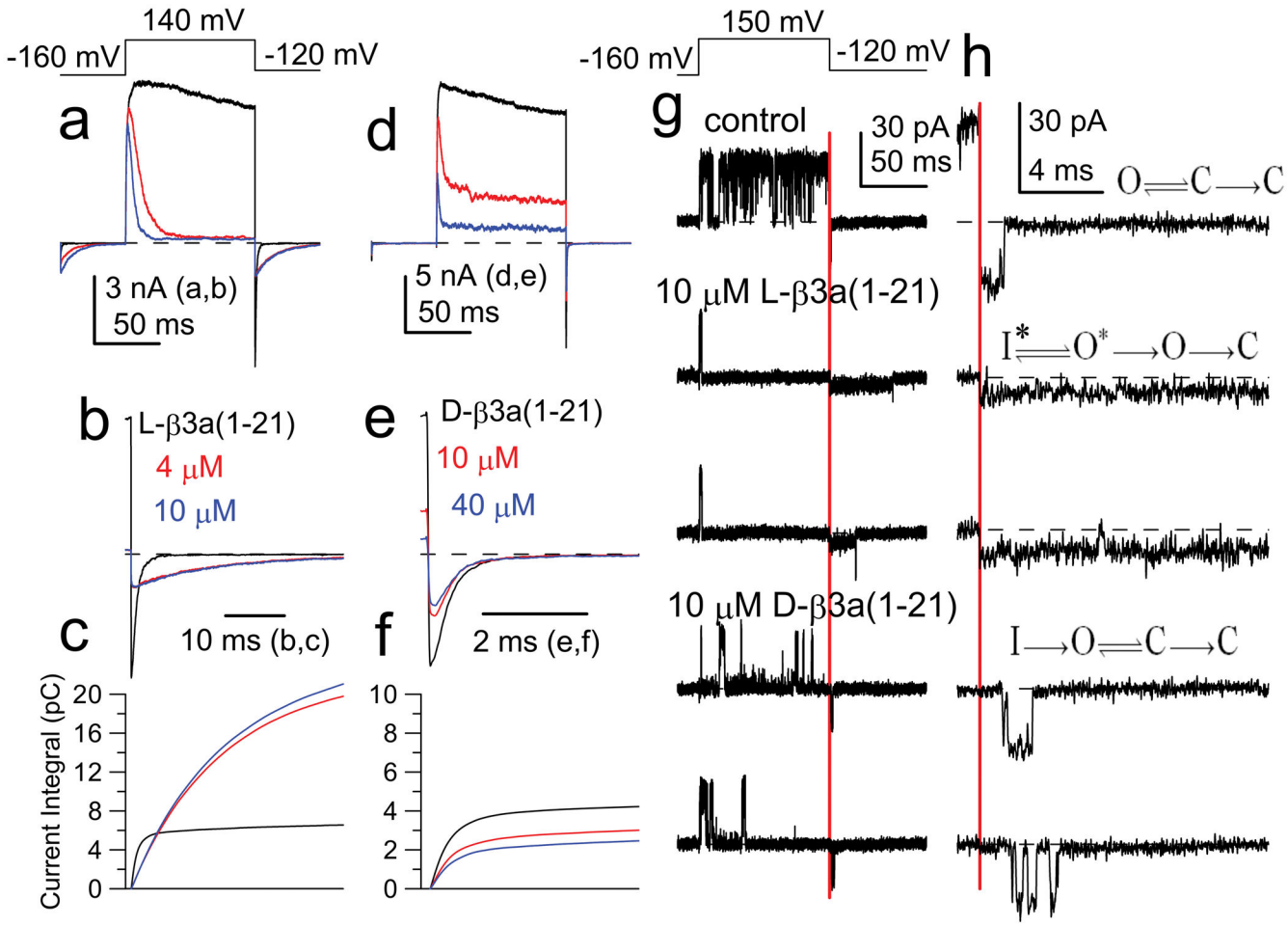

Figure 2. Intrinsically disordered D- and L- β3a peptides block BK channels, but only the L-peptide produces unique tail current behavior

(a) BK current was activated with 10 μM cytosolic Ca^{2+} with the indicated voltage protocol; 0 (black), 4 (red), and 10 (blue) μM L-β3a(1-21) peptide. **(b)** Effects of 4 and 10 μM L-peptide shown on a faster time base. **(c)** Current integrals of tail currents from panel **b**. Same time base as in **b. (d)** Currents from another patch with 0, 10, and 40 μM D-β3a(1-21) peptide. **(e)** Tail currents from (**d**) on a faster time base. **(f)** Current integrals of tail currents from panel (**e**). Same time base as (**e**). **(g)** Single BK channel (10 μM Ca^{2+}) showing control trace, two traces with 10 μM L-peptide and two traces with 10 μM D-peptide. **(h)** Faster time base examples of traces in **(g)** highlighting differences in tail current openings, consistent with indicated models. Red bar: time of repolarization.

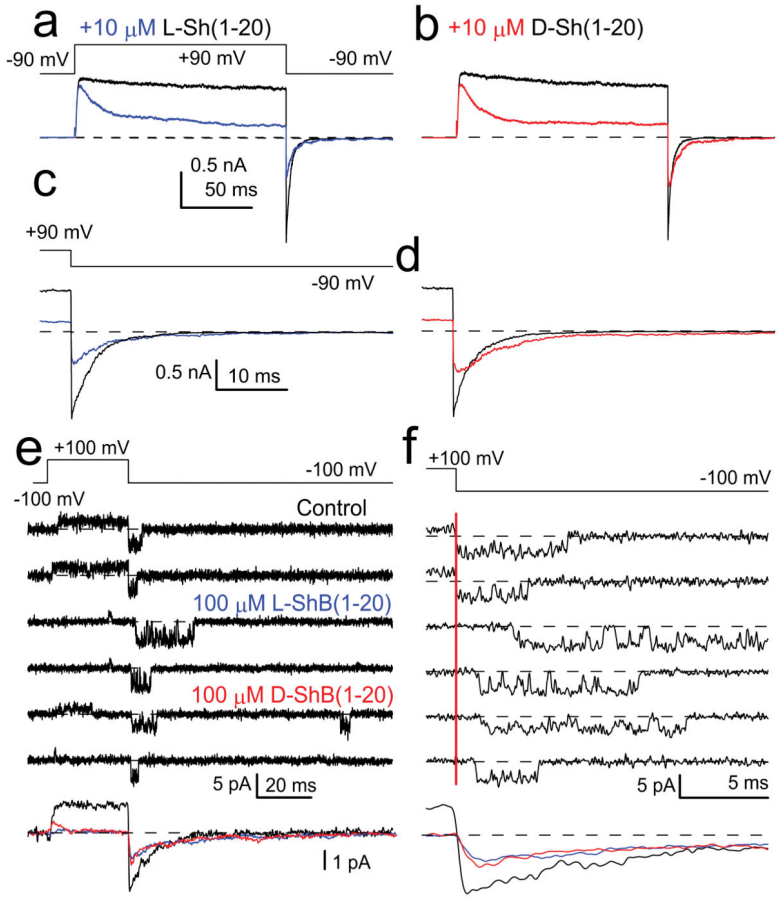

Figure 3. L- and D- Shaker peptides block *Shaker*-IR channels in a similar fashion

(a) Currents in inside-patches activated with the indicated voltage protocol with (blue) and without (black) 10 μM L-Shaker peptide. **(b)** Currents with (red) and without (black) 10 μM D-Shaker peptide. **(c)** Tail currents from **(a)** at expanded time base. **(d)** Tail currents from **(b)** at expanded time base. **(a)** and **(b)** are from the same patch. **(e)** A single Shaker-IR channel was activated and tail currents monitored during application of 100 μM L- or D-Shaker peptides. Bottom panel shows averages of 95 sweeps for no peptide (black), and 105 sweeps for D-(red) and L-peptides (blue). **(f)** Traces from **(e)** at higher time resolution. Red bar: time of repolarization. Tail openings after block by D- or L-peptide occur with an average delay of 0.51 ms (97 openings) and 0.57 ms (95 openings), respectively.

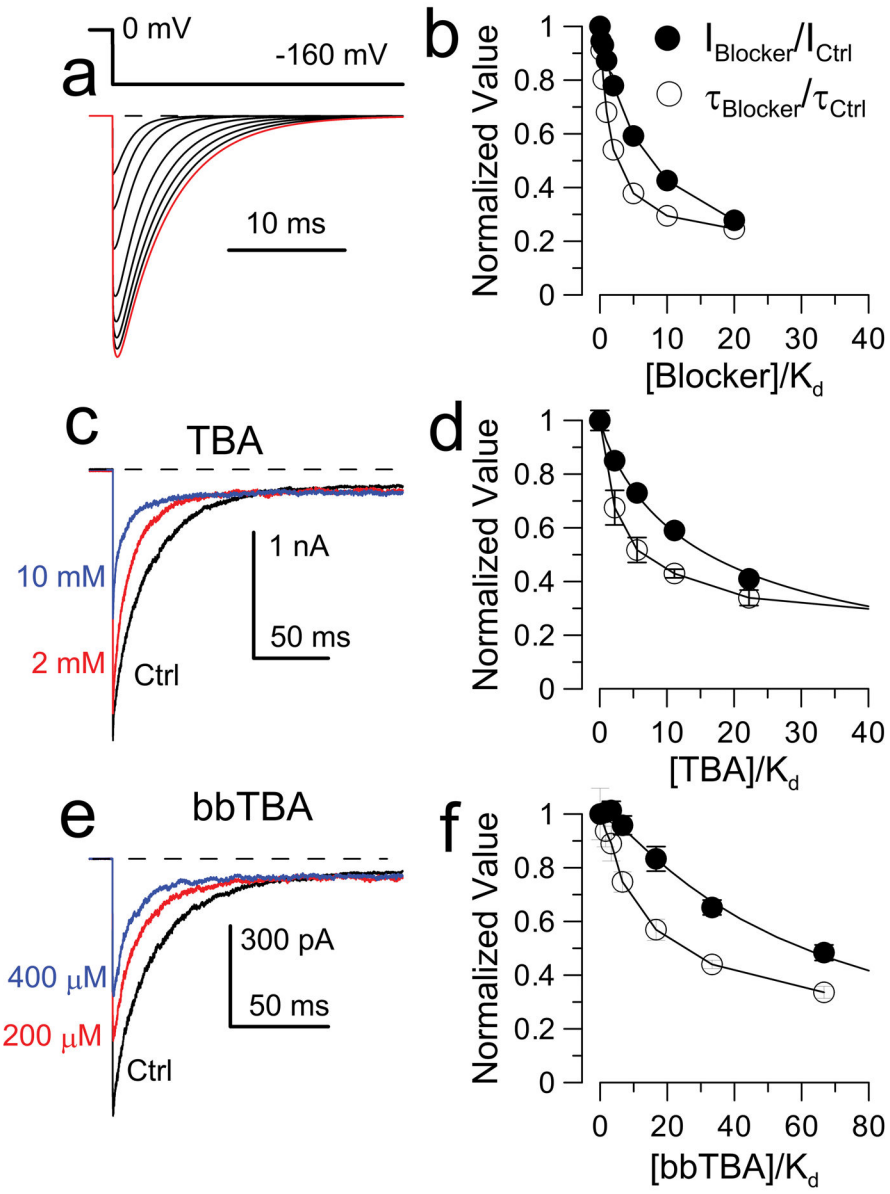

Figure 4. BK pore blockers compete with inactivation, but not N-terminus binding

(a) Tail currents simulated from Model 3 (Fig. S8a3) as [blocker] increases. **(b)** Model predictions for normalized tail current amplitude (IBlocker/ICntrl) and tail current decay (τBlocker/τCntrl) as a function of [Blocker]/Kd(0) (binding constant at 0 mV). **(c)** BK α subunits coexpressed with construct D20A (β3a N-terminus appended to β2 subunit, see Methods). Currents were activated with 10 μM Ca^{2+}, with the indicated voltage steps, along with 2 (red) or 10 (blue) mM TBA. **(d)** Effect of [TBA] on tail current amplitude and time constant plotted assuming Kd(0) for TBA is 0.9 mM. **(e)** BK α+D20A traces for control solution and with 200 and 400 μM bbTBA. (**f**) Effect of bbTBA on tail current amplitude and time constant with a Kd(0) for bbTBA block of 6 μM.